DINAME 2023 - Proceedings of the XIX International Symposium on Dynamic Problems of Mechanics,
A.S. De Paula, A.T. Fabro and M.R. Machado (Editors), ABCM.
Pirenópolis, Go, Brazil, February 26th to March 3rd, 2023

Comparative analysis between tropospheric models for GNSS positioning in Brazilian territory

Ludmila Aparecida de Oliveira[1], **Izadora Aparecida Ramos**[1], **Felipe Oliveira e Silva**[1], **Danilo Alves de Lima**[1]

[1] Universidade Federal de Lavras, Departamento de Automática.

Abstract: Global Navigation Satellite Systems (GNSS) can be applied in several areas, such as precision agriculture, vehicular navigation, intelligent/autonomous systems and air traffic control. Despite being robust, there are many sources of error that corrupt the GNSS signals used for positioning. Evaluating, controlling and mainly eliminating such sources of errors become crucial activities for these systems to reach the level of precision required in the aforementioned applications. Among the most relevant sources of error corrupting GNSS signals, there is the delay imposed on its observables when the signal propagates through the tropospheric layer of the Earth. For real-time positioning applications, the approach traditionally used to mitigate such delays is the use of empirical models based on measurements and/or estimates of atmospheric parameters. Although several models have been proposed over the years, there are few works that present a comparative study of their performance, especially in the national territory. Therefore, this work presents as a contribution, a comparative analysis, in Brazilian territory, between eight models that aim to mitigate the propagation errors of GNSS signals through the troposphere. In order to verify the effectiveness of each of these models and to determine which one presents the best performance, experimental results are presented based on GNSS data collected from reference stations belonging to the Brazilian Network for Continuous Monitoring (RBMC) of GNSS signals, which are evaluated for the Root Mean Square Errors (RMSE) of individual, horizontal and total positions. Among the models analyzed, one verifies that the one proposed by the University of Brunswick 3 (UNB3) is the one with the best performance.

Keywords: GNSS, tropospheric models, RMSE, UNB3

INTRODUCTION

The first Global Navigation Satellite Systems (GNSS) emerged in the 1970s, being composed of three segments: 1) space segment, characterized by satellites orbiting the Earth; 2) control segment, comprised of ground stations for monitoring and correcting satellite orbits and their internal (atomic) clocks; and 3) user segment, composed of receivers used for the most diverse functions. For Zhu et al. (2018), the integrity of GNSS is one of its most important performance parameters, which has attracted the interest of several sectors associated with transport systems, especially in urban areas. This is because GNSS-based urban applications have proven to be a large and attractive market, which is constantly growing. In addition to the urban area, important applications involving GNSS can also be found in agriculture and the aeronautical sector. The performance of these systems is generally analyzed according to the following criteria: accuracy, integrity, availability, and continuity.

Although GNSS are reliable and have good accuracy, there are several conditions that can cause the underlying signals to deteriorate and, consequently, cause the system to have its positioning performance impaired. The main sources of errors in GNSS, called “common mode errors”, are ephemeris prediction errors, satellite clock delay, ionospheric signal propagation delay, and troposphere signal propagation delay (Groves, 2013).

In order to ensure that the performance criteria of the application of interest are met, it is necessary to analyze the influence of these GNSS errors and, consequently, use correction models to mitigate them. Among the aforementioned common mode errors, the ones that better accommodate different compensation models are the errors related to the propagation of GNSS signals through the troposphere. As a point of convergence between most of the works dedicated to this subject, one notes that the investigations are restricted to regions close to where the GNSS receiver of interest is located and/or to the possible influence of the seasons on these errors.

Lima, Alves and Gouveia (2019), for example, evaluated the performance of Hopfield and Sastamoinen’s empirical tropospheric models in different regions of Brazil and for different atmospheric conditions, comparing them with models from the Numerical Weather Forecast. (PNT), the National Institute for Space Research (INPE) and the European Center for Medium-Range Weather Forecast (ECMWF). As verified, the PNT/INPE model showed, on average, an improvement of 29.7% and 31.7% compared to PNT/ECMWF for dry and wet days, respectively. Chuerubim and Segantine (2016), on the other hand, selected some reference stations in different seasons and geographic locations, in order to investigate the impact of Hopfield and Saastamoinen’s empirical models on high-precision geodetic positioning. The results showed that there are no statistically significant differences in the performance of these two models, although the one proposed by Saastamoinen showed an improvement in planimetry during the summer season, while the one by Hopfield showed improvements in altimetry for the data analyzed in spring, autumn, and winter.

Although the aforementioned studies/models are relevant, several other tropospheric models have been proposed in recent years, whose performance evaluation, especially in Brazilian territory, still lacks investigation. This work, therefore, presents as its main contribution a study on the performance of eight other tropospheric models, in the mitigation of tropospheric delay signals in each of the twenty-six Brazilian states, plus the Federal District. Among the investigated models, those proposed by the Standardization Agreement of the North Atlantic Treaty Organization (STANAG), Wide Area Augmentation System (WAAS), University of New Brunswick (UNB3 and UNB3m), Hartman, Collins, Magnavox, UNB3m and VMF3/GPT3 (Groves, 2013; Parkinson et al., 1996; Farrell, 2008; Leandro, Santos and Langley, 2006; Landskron and Böhm, 2016). As a metric for a proposed comparison model, the Root Mean Square Errors (RMSE) of the position of each tested GNSS reference station is used, as processed by each tropospheric compensation model.

GENERAL CONCEPTS

According to Monico (2008), the GNSS observables are subject to stochastic, systematic, and gross errors; therefore, in order to obtain reliable positioning results, the established mathematical model must be valid for the physical reality that is being described, and the sources of errors involved, well known. Systematic errors can be parameterized, reduced or even eliminated by appropriate techniques. Stochastic errors, on the other hand, do not present any deterministic relationship with the measurements and are, in general, subject to characterization only in terms of their statistical distributions. Table 1 shows some of the various GNSS errors, grouped by possible sources.

Table 1 – Sources and effects of GNSS errors.

Sources	Errors
Satélite	Orbit error
	Clock error
	Satellite antenna phase center
Signal propagation	Tropospheric refraction
	Ionospheric refraction
	Multipath
Receiver/Antenna	Clock error
	Error between channels
	Receiver antenna phase center
Season	Error in coordinates
	Earth tides
	Pole movement
	Atmospheric pressure

Adapted: Monico, 2008.

Each particular source of error can be analyzed for its effects on determining the distance between satellite and receiver. In this work, in particular, an analysis related to the error caused by the propagation delay of GNSS signals through the troposphere is presented. As explained by Farrell (2008), the troposphere is the lower part of the atmosphere, which nominally extends up to 50 km above the Earth's surface. It is essentially composed of electrically neutral particles and, for L-band signals (such as GNSS signals), it is non-dispersive. The troposphere is subject to climate-associated changes such as temperature, pressure, and humidity. As these variables affect the air mass density along the GNSS signal path and the refractive index is a function of the air mass density, they also modify the signal propagation time.

Hofmann (2008) states that one of the reasons for the existence of so many tropospheric correction models for GNSS signals is related to the difficulty of modeling water vapor. The simple use of surface measurements still does not provide the necessary precision for the so-called water vapor radiometers to be widely used in GNSS applications. These instruments, in general, measure the temperature of the sky glow via observations and thus estimate the tropospheric delay of the GNSS signal due to water vapor.

Currently, neither the GNSS control segments nor specialized institutions such as the International GNSS Service (IGS) provide real-time tropospheric delay corrections for users. Thus, it is still necessary to use mathematical models for most GNSS-based navigation applications. As a result, several authors have developed empirical models to mitigate this error, which, in general, are functions of variables such as altitude, elevation angle, time of year, etc.

Tropospheric error correction models

The equations used to implement each of the tropospheric error correction models under investigation in this work are described below.

- STANAG

The NATO Standardization Agreement (STANAG) model represents tropospheric propagation delay as a function of the elevation angle (θ_{nu}^{as}) and the orthometric heigth (H_a) of the user. The zenith delay ($\delta\rho_{TZ}$) is calculated in different ways depending on the orthometric height, as follows:

$$\delta\rho_{TZ} = [2.464 - 3.248 \times 10^{-4} H_a + 2.2395 \times 10^{-8} H_a]m \qquad Ha \leq 1,000m. \tag{1}$$

$$[2.284exp(-0.1226[10^{-3} H_a - 1]) - 0.122]m \qquad 1,000m \leq H_a \leq 9,000m. \tag{2}$$

$$0.7374exp(1.2816 - 1.424 \times 10^{-4} H_a)m \qquad 9,000m \leq Ha. \tag{3}$$

The estimated (hat symbol) slant troposphere delay ($\delta\rho_{T,a}^{s}$) for an individual signal is given by:

$$\delta\hat{\rho}_{T,a}^{s} = \frac{\delta\hat{\rho}_{TZ}}{sin\theta_{nu}^{as} + \frac{0.00143}{tan\theta_{nu}^{as} + 0.0455}} \tag{4}$$

- WAAS

In 1997, Collins and Langley proposed a hybrid neutral atmosphere model designed for Wide Area Augmentation System (WAAS) users. The WAAS model, in addition to considering the elevation angle and orthometric height, also takes into account variations in latitude (L_a) and temperature (Groves, 2013). The troposphere propagation delay estimated by the WAAS model, as well as by the STANAG model, is given in different ways depending on the orthometric height, as follows:

$$\delta\hat{\rho}_{T,a}^{s} = \frac{2.506(1 + 1.25 \times 10^{-3} \delta N_S)}{sin(\theta_{nu}^{as} + 6.11 \times 10^{-3} rad)}(1 - 1.264 \times 10^{-4} H_a)m, \qquad H_a \leq 1,500m \tag{5}$$

$$\delta\hat{\rho}_{T,a}^{s} = \frac{2.484[1 + 1.5363 \times 10^{-3} exp(-2.133 \times 10^{-4} H_a)\delta N_S]}{sin(\theta_{nu}^{as} + 6.11 \times 10^{-3} rad)} exp(-1.509 \times 10^{-4} H_a)m, \qquad H_a \geq 1,500m \tag{6}$$

where, for the northern hemisphere we have:

$$\delta N_S = 3.61 \times 10^{-3} H_a cos[2\pi(\frac{d - 152}{365})] + 0.1cos[2\pi\frac{d - 213}{365}] - 0.8225\,|L_a| \tag{7}$$

and for the southern hemisphere:

$$\delta N_S = 3.61 \times 10^{-3} H_a cos[2\pi(\frac{d - 152}{365})] + 0.1cos[2\pi\frac{d - 30}{365}] - 0.8225\,|L_a| \tag{8}$$

where d is the day of the year.

- Hartman

The Hartman model, unlike the preceding models, has much simpler calculations for tropospheric delay, considering only satellite elevation data, receiver altitude, as shown in the equation below:

$$\delta\hat{\rho}_{T,a}^{s} = \frac{2.47}{0.121 + sin\theta_{nu}} exp^{\frac{-H_a}{7518.8}} \tag{9}$$

- Collins

Very similar to Hartman's model, the tropospheric delay model proposed by Collins can be calculated as:

$$\delta\hat{\rho}_{T,a}^{s} = \frac{2.4225}{0.26 + sin\theta_{nu}} exp^{\frac{-H_a}{7492.8}} \tag{10}$$

- Magnavox

Like Hartman and Collins' models, the tropospheric delay model proposed by Magnavox (Farrel, 2008) also has a simplified calculation, as shown in the following equation:

$$\delta\hat{\rho}^{s}_{T,a} = \frac{2.208}{sin\theta_{nu}}(exp^{\frac{-H_a}{6900}} - exp^{\frac{-H_s}{6900}}) \tag{11}$$

- UNB3

In the troposphere delay model proposed by the University of New Brunswick (UNB3), the pressure, p, temperature, T, water vapor pressure, e, temperature lapse rate, β, and water vapor lapse rate, λ, are all predicted as a function of the latitude and day of the year, d, using:

$$\begin{aligned} p &= p_0(L_a) + p_\sigma(L_a)cos[2\pi(d-d_{min})/365.25] \\ T &= T_0(L_a) + T_\sigma(L_a)cos[2\pi(d-d_{min})/365.25] \\ e &= e_0(L_a) + e_\sigma(L_a)cos[2\pi(d-d_{min})/365.25] \\ \beta &= \beta_0(L_a) + \beta_\sigma(L_a)cos[2\pi(d-d_{min})/365.25] \\ \lambda &= \lambda_0(L_a) + \lambda_\sigma(L_a)cos[2\pi(d-d_{min})/365.25] \end{aligned} \tag{12}$$

where the subscript 0 denotes the mean value, the subscript σ denotes the amplitude of seasonal variation, and d_{min} is 28 in the northern hemisphere and 211 in the southern hemisphere. The UNB3 model provides values for each parameter (mean values and amplitudes of seasonal variations) in pre-established latitudes as shown in Tables 2 and 3, respectively.

Table 2 – UNB3 model: mean meteorological parameters.

Latitude (°)	p_0 (bar)	T_0 (K)	e_0 (mbar)	β_0 (K/m)	λ_0
15	1,013.25	299.65	26.31	6.30×10^{-3}	2.77
30	1,017.25	294.15	21.79	6.05×10^{-3}	3.15
45	1,015.75	283.15	11.66	5.58×10^{-3}	2.57
60	1,011.75	272.15	6.78	5.39×10^{-3}	1.81
75	1,013.00	263.65	4.11	4.53×10^{-3}	1.55

Adapted: Groves, 2013.

Table 3 – UNB3 model: seasonal amplitudes of meteorological parameters.

Latitude (°)	p_0 (bar)	T_0 (K)	e_0 (mbar)	β_0 (K/m)	λ_0
15	0.00	0.00	0.00	0.00	00
30	−3.75	7.00	8.85	0.25×10^{-3}	0.33
45	−2.25	11.00	7.24	0.32×10^{-3}	0.46
60	−1.75	15.00	5.36	0.81×10^{-3}	0.74
75	−0.50	14.50	3.39	0.62×10^{-3}	0.30

Adapted: Groves, 2013.

The aforementioned parameters (generically designated as x in the next equations) for the user in latitude are determined by interpolation parameter (mean values and amplitudes of seasonal variations) as follows:

$$\begin{aligned} x(L_a) &= x(15^\circ) && 180\,|L_a|\,/\pi \le 15^\circ \\ (2-12\,|L_a|\,/\pi)x(15^\circ) + (12\,|L_a|\,/\pi - 1)x(30^\circ) && 15^\circ \le 180\,|L_a|\,\pi \le 30^\circ \\ (3-12\,|L_a|\,/\pi)x(30^\circ) + (12\,|L_a|\,/\pi - 2)x(45^\circ) && 30^\circ \le 180\,|L_a|\,\pi \le 45^\circ \\ (3-12\,|L_a|\,/\pi)x(45^\circ) + (12\,|L_a|\,/\pi - 3)x(30^\circ) && 45^\circ \le 180 \le |L_a/\pi \le 60^\circ \\ (4-12\,|L_a|\,/\pi)x(60^\circ) + (12\,|L_a|\,/\pi - 3)x(75^\circ) && 60^\circ \le 180 \le |L_a\pi \le 75^\circ \\ x(75^\circ) && 75^\circ \le 180 \le |L_a/\pi \end{aligned} \tag{13}$$

The dry and wet (subscripts d and w, respectively) zenith delays are then calculated using:

$$\delta\hat{\rho}_{TZd} = \left(1 - \frac{\beta H_a}{T}\right)^{\frac{g}{R_d\beta}} \left(\frac{k_1 R_d p}{g_m}\right), \tag{14}$$

$$\delta\hat{\rho}_{TZw} = \left(1 - \frac{\beta H_a}{T}\right)^{\frac{(\lambda+1)g}{R_d\beta}} \left(\frac{k_2 R_d pe}{[g_m(\lambda+1) - \beta R_d]T}\right), \tag{15}$$

where, $g = 9.80665 m/s$, $R_d = 287.054 J/(kgK)$, $k_1 = 7.7604105 K/mbar$, $g_m = 9.784 m^2$ and $k_2 = 0.382 K^2$/mbar.

Lastly, the slant tropospheric delay can be calculated as:

$$\delta\hat{\rho}^s_{T,a} = \frac{\left[sin^3\theta^{nu}_{as} + (b_d + c_d)sin\theta^{nu}_{as}\right](1 + a_d + b_d + c_d + a_d c_d)}{[sin^4\theta^{nu}_{as} + (a_d + b_d + c_d)sin^2\theta^{nu}_{as} + a_d c_d]}\delta\hat{\rho}_{TZd} +$$

$$\frac{\left[sin^3\theta^{nu}_{as} + (b_w + c_w)sin\theta^{nu}_{as}\right](1 + a_w + b_w + c_d + a_w c_w)}{[sin^4\theta^{nu}_{as} + (a_w + b_w + c_w)sin^2\theta^{nu}_{as} + a_w c_w]}\delta\hat{\rho}_{TZw} \tag{16}$$

where

$$a_d = 1.18972 \times 10^{-3} - 2.6855 \times 10^{-5} H_a + 1.0664 \times 10^{-4} cosL_a$$

$$b_d = 3.5716 \times 10^{-4} \qquad c_d = 8.2456 \times 10^{-2}$$

$$a_w = 6.1120^{-4} - 3.5348 \times 10^{-5} H_a + 1.526 \times 10^{-5} cos(L_a) \tag{17}$$

$$b_w = 1.8576 \times 10^{-3} \qquad c_w = 6.2741 \times 10^{-2}$$

- UNB3m

UNB3m is a neutral atmosphere-based tropospheric delay model developed by UNB. As UNB3, its algorithm is based on the prediction of meteorological parameter values for a given location, i.e., it depends on the latitude and altitude of the location, and day of the year. These parameters are used to calculate hydrostatic (dry) and non-hydrostatic (wet) zenith delays using Saastamoinen models. Slanted delays (and/or lag rates) are then determined using Niell mapping functions (or mapping function rates in the case of lag rates) (Leandro et al., 2006). UNB3m is actually a modified version of UNB3.

Then, dry and wet zenith tropospheric delays can be calculated according to:

$$\delta\hat{\rho}_{TZd} = \frac{10^{-6} k'_1 R_d}{g_m} p \left(1 - \frac{\beta H}{T}\right)^{\frac{g}{R_d\beta}}, \tag{18}$$

$$\delta\hat{\rho}_{TZw} = \frac{10^{-6}(T_m k'_2 + k_3) R_d}{g_m \lambda' - \beta R_d} \frac{e}{T} \left(1 - \frac{\beta H}{T}\right)^{\frac{(\lambda+1)g}{R_d\beta} - 1} \tag{19}$$

where, k'_1, k'_2 and k_3 are refraction constants with values of 77.6 K $mbar^-1$, 16.6 K $mbar^-1$ and 377600 K $mbar^-1$ respectively, and:

$$g_m = 9.784(1 - 2.66 \times 10^{-3} cos(2L_a) - 2.8 \times 10^{-7} \tag{20}$$

$$T_m = T(1 - \frac{\beta R_d}{g_m \times (\lambda + 1)}) \tag{21}$$

The total slant delay lastly, can be calculated according to:

$$\delta\hat{\rho}^s_{T,a} = m_d \times \delta\hat{\rho}_{TZd} + m_w \times \delta\hat{\rho}_{TZw} \tag{22}$$

where, m_d and m_w represent hydrostatic and non-hydrostatic mapping functions (Niell, 1996), which was developed to avoid UNB3's problematic relative humidity (RH) values. Alternatively, UNB3m proposes tabulated values for the relative humidity, in replacement to UNB3's water vapor pressure estimates, as shown in Table 4.

Table 4 – UNB3m: mean and seasonal amplitudes of relative humidity

	Relative Humidity (%)	
Latitude	Average	Amplitude
15	75.0	0.0
30	80.0	0.0
45	76.0	-1.0
60	77.5	-2.5
75	82.5	2.5

Table 4 should replace the columns for water vapor pressure in the UNB3's Tables 2 and 3, where the final Tables 2 and 3 is then transformed into water vapor pressure. This conversion can be performed following International Earth Rotation and Reference Frame Services (IERS) conventions as follows:

$$e_0 = \frac{RH}{100} e_s f_w \tag{23}$$

where the saturation vapor pressure, e_s, can be calculated as:

$$e_s = 0.01 exp(1.2378847 \times 10^{-5} T^2 - 1.9121316 \times 10^{-2} T + 33.93711047 - 6.343165 \times 10^3 T^{-1} \tag{24}$$

and the enhancement factor, f_w, can be determined as follows:

$$f_w = 1.00062 + 3.14 \times 10^{-6} P + 5.6 \times 10^7 (T 273.15)^2. \tag{25}$$

- VMF3/GPT3:

The Vienna Mapping Functions 3 (VMF3) are a new approach that aims to refine the discrete mapping function Vienna Mapping Functions 1 (VMF1) (Böhm et al., 2006). The Global Pressure and Temperature 3 (GPT3), in turn, is a new empirical model that works on a global grid, and that is usually based on the same data as VMF3. Its main components are wet and hydrostatic empirical mapping function coefficients derived from special averaging techniques of the respective VMF3 (discrete) data. In addition, GPT3 also contains a set of meteorological quantities that are adopted as-is from its predecessor, GPT2. Thus, GPT3 represents a very comprehensive troposphere model that can be used for a number of geodetic, meteorological and climatological purposes and is fully consistent with VMF3 (Landskron and Böhm, 2016).

Detailed description of VMF3/GPT3 implementation is not included in this work due to space constraints. The interested reader is invited to refer directly to (Landskron and Bohm, 2016) though.

METHODOLOGY

In order to carry out a comprehensive analysis of the performance of the tropospheric delay models under investigation, GNSS data from receivers located in all Brazilian states plus the Federal District were selected. The observation and navigation GNSS data, in Receiver INdependent EXchange 2 (RINEX 2) format, were collected for the same day and time, from reference stationsbelonging to the Brazilian Network for Continuous Monitoring (RBMC) of GNSS systems (Figure 1).

The RBMC consists of a set of geodetic stations, equipped with high performance GNSS receivers, which provide, once a day or in real time, observations for the determination of geographic coordinates. Each station has a geodesic receiver and antenna, an Internet connection and a constant supply of electrical power that enables the station's continuous operation. The coordinates of the RBMC stations are another important component in the composition of the final results of the surveys referenced to it. In this aspect, the great advantage of the RBMC is that all its stations are part of the SIRGAS (Geocentric Reference System for the Americas), reference network, whose final coordinates have an accuracy of the order of ± 5 mm, configuring itself as one of the most accurate networks in the world.

After collection, the data were post-processed (via GNSS positioning algorithms implemented by the authors), in a Matlab environment, in order to determine the Root Mean Square Errors (RMSE) of position in the North (N), East (E) and Down (D) axes, as well as in the horizontal and total directions. The mentioned process follows the steps as shown in the diagram in Figure 2. This approach was used for each set of data collected and the RMS values obtained were stored in order to perform the comparison between the tropospheric models.

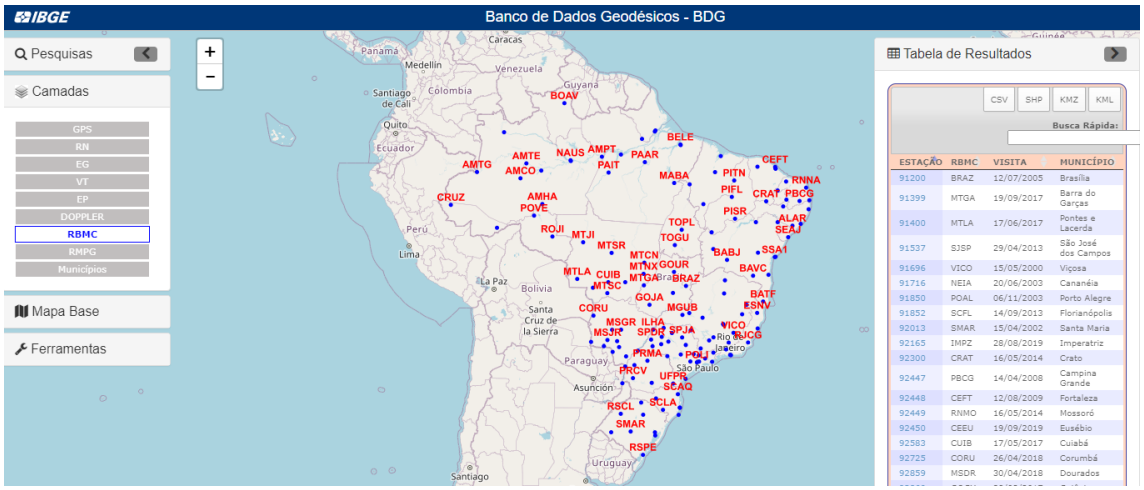

Figure 1 – RBMC reference stations.

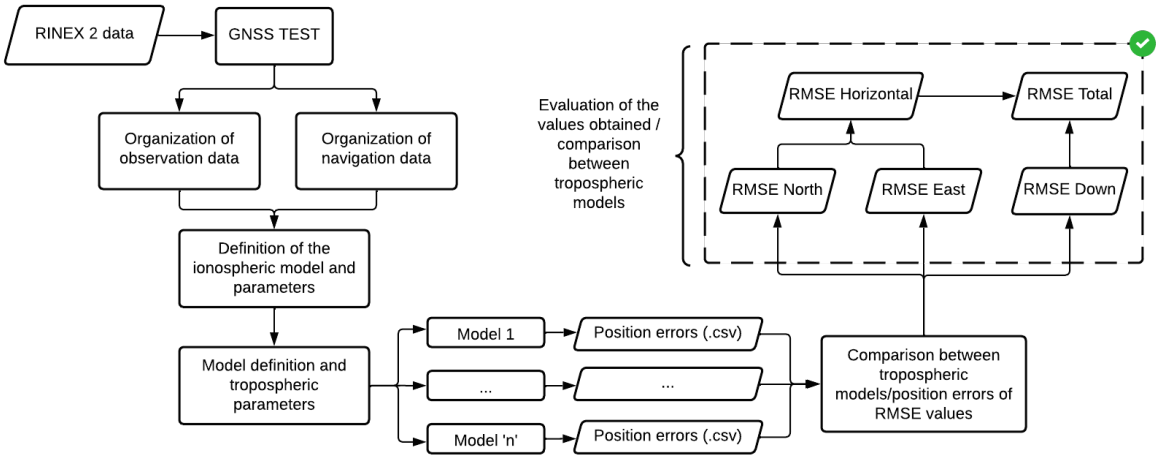

Figure 2 – Block diagram: GNSS TEST.

RESULTS AND DISCUSSIONS

In order to illustrate how the comparison between the investigated tropospheric models took place, data from RMBC's reference station located in the city of Lavras-MG (MGLA) were initially used. Figure 3 illustrates the behavior of position errors along the NED axes (North, East and Down) for the eight analyzed models. As can be seen, the UNB3 model is the one with the most discrepant behavior (in relation to the others), resulting in an improvement in positioning in the north direction, but deterioration in the east and down.

Only via graphical analysis of the individual position errors (on each axis) it is not possible to determine the best tropospheric correction model. Therefore, as an additional metric for this determination, the RMSE values of their composition into the horizontal (north and east) and total (north, east and down) were also calculated (Table 5). As can be seen, the RMSE values of MGLA horizontal and total position show an improved global performance of UNB3, in comparison to the others, despite its position deterioration exclusively in the east direction. In order to show the behavior of the combined horizontal and total position RMSE, Figure 4 presents the distribution of these errors according to each of the eight models analyzed.

The same analysis described above was extended to other GNSS bases, belonging to the RBMC, and located in each of the other Brazilian states (plus the Federal District). By analyzing the bases individually according to horizontal and total position RMSE, we have identified and classified the three tropospheric error mitigation models that presented the best performance, as seen in Table 6.

In order to globally verify, the behavior of the investigated tropospheric models, Table 7 lists the number of times/bases in which each tropospheric model under investigation performed as the best, second best and third best, respectively (in terms of horizontal and total position RMSE values). As can be seen, among the investigated models, the one proposed by

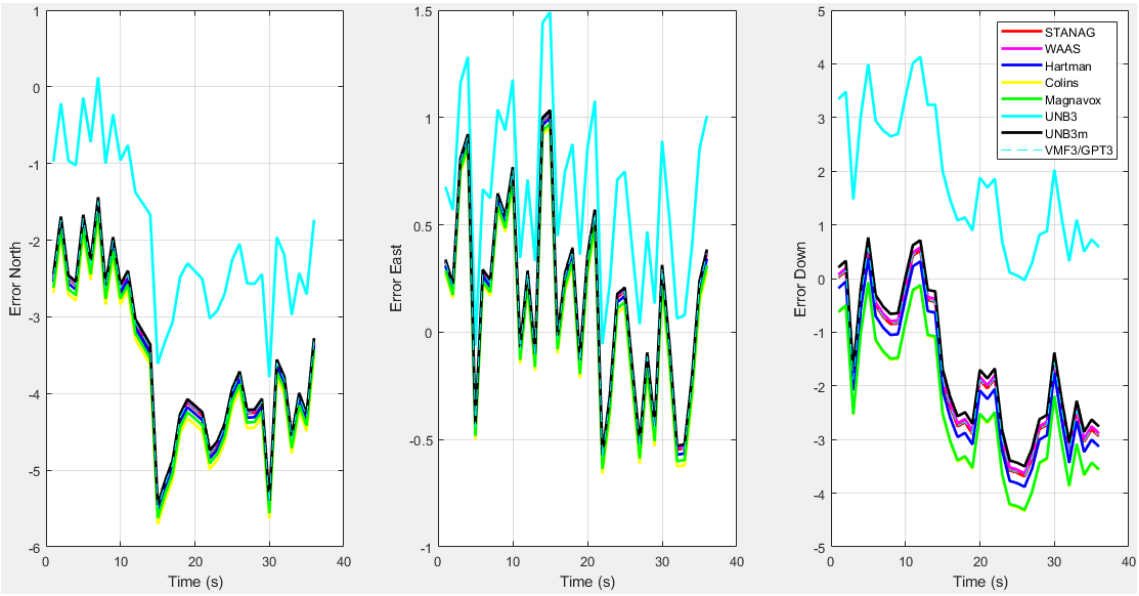

Figure 3 – Position errors for each NED axis.

Table 5 – RMSE values of position errors for the MGLA base (in meters).

MODEL	NORTH	EAST	DOWN	HORIZONTAL	TOTAL
STANAG	3,77	0,46	2,21	3,80	4,39
WAAS	3,75	0,47	2,16	3,78	4,36
Hartman	3,82	0,46	2,37	3.85	4,53
Collins	3,96	0,45	2,76	3.99	4,85
Magnavox	3,89	0,45	2,74	3,91	4,78
UNB3m	2,18	0,76	2,20	2,31	3,19
UNB3m	3,73	0,47	2,06	3,76	4,29
VFM3/GPT3	3,77	0,46	2,21	3,79	4,39

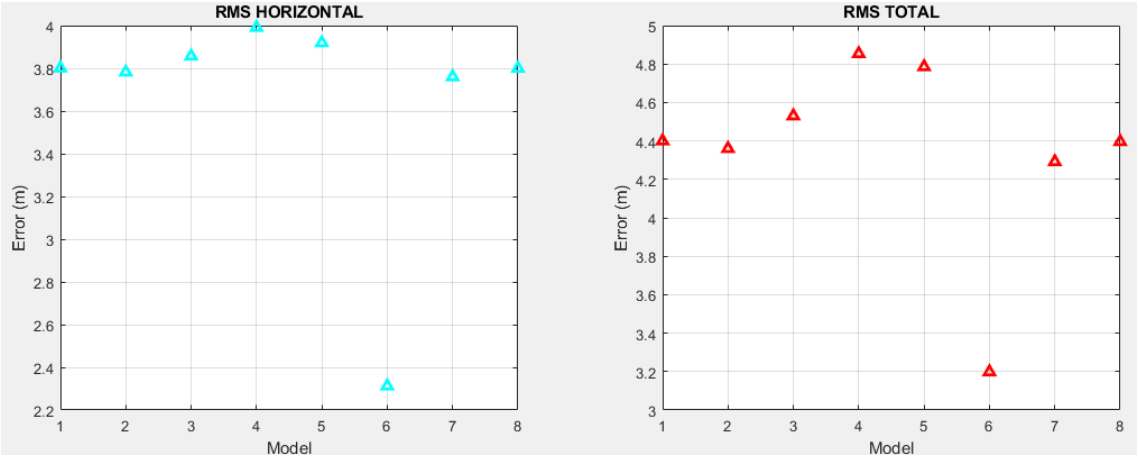

Figure 4 – Position errors for each NED axis.

UNB3 was the one that presented the best performance for most of the analyzed bases, having been followed by UNB3m and VMF3/GPT3, respectively. This can be explained by the fact that the UNB3, UNB3m and VMF3/GPT3 involve more complete calculations (in comparison to the remaining methods), being, hence, able to more accurately predict the tropospheric delays acting on GNSS signals. It is interesting to notice however, that UNB3m performed worse than UNB3, even though the former has been conceived to overcome limitations of the latter. If one consults the original work by Leandro et al. (2006), one verifies that the main drawback of UNB3 (that motivated the proposition of UNB3m) lied on the fact that UNB3 overestimates the relative humidity in locations close to the Earth poles. As Brazilian territory is far from the latter, that can explain why UNB3 performed better than UNB3m in the conducted experiments.

Table 6 – Classification of tropospheric models according to Hhorizontal and total position RMSE.

Base	Localization Municipality-State	Horizontal RMSE			Total RMSE		
		Best Model	*2° Best Model*	*3° Best Model*	*Best Model*	*2° Best Model*	*3° Best Model*
ALMA	Maceió-AL	Collins	Magnavox	Hartman	UNB3	UNB3m	VMF3/ GPT3
AMUA	Manaus-AM	UNB3	VMF3/ GPT3	UNB3m	Magnavox	Collins	Hartman
APMA	Macapá-AP	Collins	Magnavox	Hartman	Magnavox	Collins	Hartman
BELE	Belém-PA	Collins	Magnavox	Hartman	Magnavox	Hartman	Collins
BOAV	Boa Vista-RR	Collins	Magnavox	Hartman	Magnavox	Collins	Hartman
BRAZ	Brasília-DF	Collins	Magnavox	Hartman	UNB3m	VMF3/ GPT3	WAAS
CEFE	Vitória-ES	UNB3	UNB3m	VMF3/ GPT3	UNB3	UNB3m	VMF3/ GPT3
CEFT	Fortaleza-CE	UNB3	VMF3/ GPT3	UNB3m	UNB3	VMF3/GPT3	UNB3m
GOGY	Goiânia-GO	UNB3m	WAAS	VMF3/ GPT3	Magnavox	Collins	Hartman
MGBH	Belo Horizonte-MG	UNB3	UNB3m	WAAS	UNB3	UNB3m	VMF3/ GPT3
MSAQ	Aquidauana-MS	UNB3	UNB3m	VMF3/ GPT3	UNB3	UNB3m	VMF3/ GPT3
MTSC	Barão de Melgaço-MT	Collins	Magnavox	Hartman	UNB3	UNB3m	VMF3/ GPT3
ONRJ	Rio de Janeiro-RJ	UNB3	UNB3m	VMF3/ GPT3	UNB3	UNB3m	VMF3/ GPT3
PBJP	João Pessoa-PB	Collins	Hartman	STANAG	Magnavox	Hartman	Collins
PERC	Recife-PE	WAAS	UNB3	Magnavox	Magnavox	Hartman	Collins
PITN	Terezina-PI	UNB3	UNB3m	VMF3/ GPT3	UNB3	UNB3m	VMF3/ GPT3
POAL	Porto Alegre-RS	UNB3	UNB3m	WAAS	UNB3	UNB3m	VMF3/ GPT3
POVE	Porto Velho-RO	UNB3	UNB3m	VMF3/ GPT3	STANAG	WAAS	Hartman
RIOB	Rio Branco-AC	UNB3	UNB3m	VMF3/ GPT3	UNB3	UNB3m	VMF3/ GPT3
RNNA	Natal-RN	UNB3	UNB3m	VMF3/ GPT3	Magnavox	Hartman	Collins
SALU	São Luiz-MA	UNB3	UNB3m	VMF3/ GPT3	UNB3	UNB3m	VMF3/GPT3
SAVO	Salvador-BA	UNB3	UNB3m	VMF3/ GPT3	UNB3	VMF3/ GPT3	UNB3m
SCFL	Florianópolis-SC	UNB3	UNB3m	VMF3/ GPT3	UNB3	VMF3/ GPT3	UNB3m
SEAJ	Aracajú-SE	Magnavox	Collins	Hartman	Magnavox	Hartman	Collins
SPJA	Jaboticabal-SP	UNB3	UNB3m	WAAS	UNB3m	WAAS	VMF3/ GPT3
TOPL	Palmas-TO	UNB3	UNB3m	VMF3/ GPT3	UNB3	VMF3/ GPT3	UNB3m
UFPR	Curitiba-PR	UNB3	UNB3m	WAAS	UNB3	VMF3/ GPT3	WAAS

CONCLUSION

This work investigated, in terms of position RMSE values, the performance for different empirical models of tropospheric delay compensation in GNSS signals. Among the investigated models, those proposed by STANAG, WAAS, Hartman, Collins, Magnavox, UNB3, UNB3m and VMF3/GPT3 stand out. Experimental results, carried out with GNSS

Table 7 – Number of bases in which each of the models performed best (in terms of horizontal and total position RMSE values).

MODELO	HORIZONTAL			TOTAL		
	Best Model	*2° Best Model*	*3° Best Model*	*Best Model*	*2° Best Model*	*3° Best Model*
STANAG	0	0	1	1	0	0
WAAS	1	1	4	0	2	2
Hartman	0	1	7	0	0	0
Collina	7	1	0	5	4	0
Magnavox	1	6	1	4	5	0
UNB3	17	1	0	15	0	10
UNB3m	1	15	2	2	13	2
VMF3/GPT3	0	2	12	0	3	13

data collected from stations belonging to the RBMC, and spread across each of the Brazilian states (including the Federal District) indicated the best performance of the UNB3 model for GNSS positioning purposes, followed by the UNB3m and VMF3/GPT3 models. As a possible future work, the authors intend to analyze the performance of each tropospheric model as a function of the time of day, and season of the year. Additionally, the use of the tropospheric models in the scope of Real-Time Precise Point Positioning (RT-PPP) is also a topic worthy of investigation.

ACKNOWLEDGMENTS

This work was supported in part by the Research Development Foundation (FUNDEP - ROTA 2030), under grant/award number 27192.02.02/2021.01.00; in part by the National Council for Scientific and Technological Development (CNPq), under grant/award number 313160/2019-8; in part by the Brazilian Agricultural Research Corporation (EMBRAPA), under grant/award number 212-20/2018; and in part by the Minas Gerais Research Foundation (FAPEMIG), under grants/awards numbers APQ-01449-17 and APQ-04659-22.

The authors also thank the Graduate Program on Systems Engineering and Automation (PPGESISA) of the Federal University of Lavras (UFLA) for supporting the research.

REFERENCES

BOEHM, J.; BIRGI, W. and HARALD, S.Troposphere mapping functions for GPS and very long baseline interferometry from European Centre for Medium-Range Weather Forecasts operational analysis data. JOURNAL OF GEOPHYSICAL RESEARCH, VOL. 111, B02406, doi:10.1029/2005JB003629.

FARREL, J. A. Aided Navigation: GPS with High Rate Sensors. [S.l.]: The McGraw-Hill Companies, Inc., 2008.

GROVES, P. D. Principles of GNSS, Inertial, and Multisensor Integrated Navigation Systems. London: Artech House Remote Sensing Library, 2013.

HOFMANN, W. B.; LICHTENEGGER, H. e WASLE, E. GNSS – Global Navigation Satellite Systems GPS, GLONASS, Galileo, and more. Springer−Verlag Wien, 2008.

HUERUBIM, M. K. and SEGANTINE, P. C. L. O IMPACTO DOS MODELOS TROPOSFÉRICOS NO POSICIONAMENTO GNSS DE ALTA PRECISÃO EM DIFERENTES ÉPOCAS E ESTAÇÕES DO ANO. Revista de Engenharia e Tecnologia, V. 8, No. 2, Ago/2016.

LEANDRO, R.; SANTOS, M.and LANGLEY, R. B. UNB neutral atmosphere models: Development and performance. In Proceedings of the ION NTM, Monterey, CA, USA, 18–20 January 2006.

LIMA, T. M. A.; ALVES, D. B. M. and GOUVEIA, T. A .F. MODELAGEM TROPOSFÉRICA: ESTUDO E ANÁLISE DE DIFERENTES MODELOS. SIMPÓSIO BRASILEIRO DE SENSORIAMENTO REMOTO, Abril de 2019.

MONICO, J. F. G. Posicionamento pelo GNSS: Descrição, Fundamentos e Aplicações. São Paulo; Editora UNESP, 2008.

NIELL, A.E. "Global Mapping Functions for the Atmosphere Delay at Radio Wavelengths." Journal of Geophysical Research, Vol. 101, 1996.

PARKINSON, B. W. et al. J J. Global Positioning System: Theory and Applications. [S.l.]: American Institute of Aeronautics and Astronautics, 1996.

IBGE. Available in $< https://www.ibge.gov.br/geociencias/informacoes-sobre-posicionamento-geodesico/rede-geodesica/16258-rede-brasileira-de-monitoramento-continuo-dos-sistemas-gnss-rbmc.html?=t=sobre >$ Access: June 2022.

ZHU, Ni et al. GNSS Position Integrity in Urban Environments: A Review of Literature. IEEE TRANSACTIONS ON INTELLIGENT TRANSPORTATION SYSTEMS, v. 19, n. 9, SEPTEMBER 2018.